

# Anti-T-lymphocyte globulin exposure is associated with acute graft-versus-host disease and relapse in pediatric acute lymphoblastic leukemia patients undergoing hematopoietic stem cell transplantation: a multinational prospective study

Lisa V.E. Oostenbrink,<sup>1</sup> Erik G.J. von Asmuth,<sup>1</sup> Cornelia M. Jol-van der Zijde,<sup>1</sup> Anja M. Jansen-Hoogendijk,<sup>1</sup> Carly Vervat,<sup>1</sup> Robbert G.M. Bredius,<sup>1</sup> Maarten J.D. van Tol,<sup>1</sup> Marco W. Schilham,<sup>1</sup> Petr Sedlacek,<sup>2</sup> Marianne Ifversen,<sup>3</sup> Adriana Balduzzi,<sup>4</sup> Peter Bader,<sup>5</sup> Christina Peters<sup>6</sup> on behalf of the FORUM study group, Dirk Jan A.R. Moes<sup>7#</sup> and Arjan C. Lankester<sup>1#</sup>

<sup>1</sup>Willem-Alexander Children's Hospital, Leiden University Medical Center, Leiden, the Netherlands; <sup>2</sup>Motol University Hospital, Prague, Czech Republic; <sup>3</sup>Department of Children and Adolescents Medicine, Copenhagen University Hospital Rigshospitalet, Copenhagen, Denmark; <sup>4</sup>Pediatric Hematopoietic Stem Cell Transplant Unit, Fondazione IRCCS San Gerardo dei Tintori, School of Medicine and Surgery, Milano-Bicocca University, Monza, Italy; <sup>5</sup>University Hospital Frankfurt, Frankfurt am Main, Germany; <sup>6</sup>St. Anna Children's Hospital, Children's Cancer Research Institute, Vienna, Austria and <sup>7</sup>Department of Clinical Pharmacy & Toxicology, Leiden University Medical Center, Leiden, the Netherlands

<sup>#</sup>DJARM and ACL contributed equally as senior authors.

**Correspondence:** L.V.E. Oostenbrink  
[V.E.Oostenbrink@LUMC.nl](mailto:V.E.Oostenbrink@LUMC.nl)

A.C. Lankester  
[A.Lankester@LUMC.nl](mailto:A.Lankester@LUMC.nl)

**Received:** November 17, 2023.

**Accepted:** April 26, 2024.

**Early view:** May 9, 2024.

<https://doi.org/10.3324/haematol.2023.284632>

©2024 Ferrata Storti Foundation

Published under a CC BY-NC license



## Supplementary appendix

**Supplement to: Anti-T-lymphocyte globulin exposure is associated with acute Graft-versus-Host Disease and relapse in pediatric acute lymphoblastic leukemia patients undergoing hematopoietic stem cell transplantation: a multinational prospective study**

### **ATLG exposure affects aGvHD and relapse in pediatric ALL**

Lisa V.E. Oostenbrink, Erik G.J. von Asmuth, Cornelia M. Jol-van der Zijde, Anja M. Jansen-Hoogendijk, Carly Vervat, Robbert G.M. Bredius, Maarten J.D. van Tol, Marco W. Schilham, Petr Sedlacek, Marianne Ifversen, Adriana Balduzzi, Peter Bader, Christina Peters; on behalf of the FORUM study group, Dirk Jan A.R. Moes, Arjan C. Lankester

**Corresponding authors:** Lisa V.E. Oostenbrink, Leiden University Medical Centre, Laboratory of Pediatric Immunology, WAKZ, P3-024; P.O. Box 9600, 2300 RC Leiden, The Netherlands. Phone number: 0031-715263331. E-mail: [V.E.Oostenbrink@LUMC.nl](mailto:V.E.Oostenbrink@LUMC.nl)

Arjan C. Lankester, Leiden University Medical Centre, WAKZ, J-06-138; P.O. Box 9600, 2300 RC Leiden, The Netherlands, Phone number 0031-715264871, E-mail [A.Lankester@LUMC.nl](mailto:A.Lankester@LUMC.nl)

<b>Table of contents</b>	<b>Page</b>
Supplemental methods	
Sampling and total and active ATLG analysis	4
Pharmacokinetic modelling	4-5
Supplemental results	
Pharmacokinetic model development and model evaluation	6
Supplemental tables	
Table S1 Number of patients included according to country	7
Table S2 Evaluated covariates for model development	7
Table S3 Model estimated pharmacokinetic metrics	8
Table S4 Model building process	9-10
Table S5 Results of the logistic regression predicting grade II-IV aGvHD and AUC-ROC curves	10
Table S6 Patient characteristics low and high ATLG exposure group	11-12
Table S7 Patient characteristics low, intermediate and high ATLG exposure group	13-14
Table S8 Association between patient, disease and transplant characteristics and ATLG exposure	15
Table S9 Results of the multivariate analyses of aGvHD and relapse rate	16
Table S10 Bivariate analysis of graft source and ATLG exposure on relapse rate and death	17
Table S11 Bivariate analysis of TBI and ATLG exposure on relapse rate	17
Table S12 Co-occurrence of relapse and mortality	17
Supplemental figures	
Figure S1 Final pharmacokinetic model structure	18
Figure S2 Impact of bodyweight as covariate on inter-individual variability of ATLG clearance and central volume of distribution before and after model inclusion	19
Figure S3 Goodness of fit plots for the final PK model	20
Figure S4 Normalized Prediction Distribution Errors plots	21
Figure S5 Prediction corrected visual predictive check of the final pharmacokinetic model on normal scale	21

Figure S6 Prediction corrected visual predictive check of the final pharmacokinetic model on lognormal scale	22
Figure S7 Correlation plot of the ATLG exposure metrics	23
Figure S8 Kaplan-meier curves for overall, event-free and relapse-free survival	24
Figure S9 Relapse and relapse-free survival in patients with or without aGvHD	25
Figure S10 Effect of ATLG exposure on relapse-rate in MRD positive vs. negative patients	26
Figure S11 Engraftment and ATLG exposure	27
Figure S12 Competing risk cumulative incidence curves for EBV, CMV and HadV	28
Figure S13 Immune reconstitution at 4, 8 and 12 weeks post-HSCT	29
List of participating institutions	30-31
Final population PK model code	32-34
Shiny ATLG Population PK model simulation application	35-37
Supplemental references	38
Individual plots per patient with observed and individual model predicted concentration-time curves	39



## Supplemental methods

### Sampling and ATLG measurements

For ATLG PK assessment, samples were taken before the start of the first dose, 15 minutes after the last dose and at one, two, three- and four-weeks post-transplantation. To improve model estimation on ATLG clearance in between dosing, the concentration at the day of transplantation and the peak and trough concentrations taken 15 minutes after each dose and just before the next dose were determined in 16 patients. Serum samples were cryopreserved until bioanalysis.

For total ATLG (rabbit IgG) analysis, enzyme-linked immunosorbent assay (ELISA) microtiter plates were coated with goat anti-rabbit IgG adsorbed for human IgG (Jackson Europe, Suffolk, UK). After blocking and washing, a rabbit IgG standard curve (ATG Thymoglobulin, range 4-250 ng/mL) and diluted patient's sera (2-fold dilutions with a dilution of at least 1:100) were incubated for 1 hour, followed by washing and incubation with alkaline phosphatase-conjugated goat anti-rabbit IgG adsorbed for human IgG (Jackson Europe)<sup>1,2</sup>.

Active ATLG analysis was performed using HUT-78 T-cells. Cells were incubated with diluted patient's serum/plasma, starting dilution dependent on the result of the total ATLG assay and often multiple dilutions for one sample were analysed (as example, for a sample taken after the last ATLG dose we analysed a 10, 20 and a 40 times dilution of the sample). For the reference curve, HUT-78 cells were incubated with known concentrations of ATG Thymoglobulin (range 0.024 to 25 µg/mL, 1 µg Thymoglobulin was arbitrarily set to contain 1 AU of active ATG). Afterwards, cells were washed and incubated with Alexa Fluor 647 labelled goat anti-rabbit (Life Technologies, Carlsbad, CA, USA). Finally, cells were washed and analysed by flow cytometry on a FACSCalibur™ Flow Cytometer (Becton Dickinson Biosciences, Franklin Lakes, NJ, USA). Mean fluorescence intensities (MFI) achieved at the different standard dilutions were log-log plotted against the active ATG/ATLG concentrations to calculate a standard curve. The concentration of active ATLG in patient samples was recalculated from the reference curve. The lower limit of quantification for active ATLG was 0.1 AU/mL, the lower limit of detection was 0.01 AU/ml. All measurements were performed at least in duplicate.

Historically ATG Thymoglobulin reference curves were used in our lab, also for measuring ATLG concentrations. Therefore, we first compared Thymoglobulin and Grafalon reference curves. This demonstrated that relative to the Thymoglobulin curve, the Grafalon curve was parallel shifted with a factor of 2.3<sup>1</sup>, confirming previously published data that Grafalon contains less active ATLG per µg rabbit IgG than Thymoglobulin<sup>3</sup>.

All patient samples were screened for the presence of anti-rabbit antibodies (IgM, IgA and IgG) using an ELISA assay. Plates were coated with ATG and after blocking, patient sera were applied. Bound anti-rabbit antibodies were detected with alkaline phosphatase-conjugated goat anti-human IgM (309-055-095; 1:5000 diluted; Jackson Europe), goat anti-human IgA (309-055-011; 1:1000 diluted; Jackson Europe) or rabbit anti-human IgG (309-055-008; 1:5000 diluted; Jackson Europe), absorbed for rabbit IgG. In 24 samples of 14 patients anti-ATLG antibodies were detected. These samples were labelled and during model development we assessed if exclusion of the active ATG values of these samples/patients influenced our POPPK model, since our group previously published the influence of IgG anti-ATG antibodies on Thymoglobulin clearance. No effect was seen on the final model POPPK parameter estimates (data not shown). Therefore, we did not exclude these samples.

### Population pharmacokinetic modelling

A nonlinear mixed-effects model was developed to estimate the POPPK parameters of active ATLG in pediatric HSCT patients using the first-order conditional estimation with interaction (FOCE-I) estimation method. For this purpose, the non-linear mixed effects software package NONMEM version 7.4.4 (Icon Hanover, MD, USA) was used<sup>4-6</sup>, with Pirana 2.9.8, RStudio 1.4.1717 and R 3.6.3 (RStudio Inc., Boston, MA, USA)<sup>7</sup> as modelling environment and data visualization<sup>8,9</sup>, respectively. Logarithmic transformation of active ATLG data was initially explored, however this did not improve parameter estimation. Handling of concentrations below the limit of quantification for the assay was evaluated using different methods: M6: set at half the limit of quantification, with any subsequent measurements below the limit of quantification being removed, M3: using the Laplacian estimation method in NONMEM. And keeping all the data with a residual error model consisting of a combined proportional and additive error.

Clearance of antibodies, such as ATLG, is assumed to be a combination of both linear (drug clearance independent of the ATLG levels, non-specific binding) and saturable target-mediated elimination (non-linear)<sup>10</sup>. Therefore, for the structural model one- and two-compartmental models with and without linear and nonlinear (Michaelis-Menten) clearance were explored to find the optimal fit for the concentration-time data. Inter-occasion variability was explored on all parameters involved in elimination to detect potential time-dependency.

Throughout the model building process, candidate models were evaluated for a decrease in objective function value (OFV [-2 log likelihood]). A drop of  $\geq 6.63$  ( $p < 0.01$ , with 1 degree of freedom, Chi-square distribution) in OFV was considered statistically significant. Additionally, model selection was based on goodness-of-fit (GOF) plots in which observed concentration vs. individual- and population- predicted concentrations, the conditional-weighted residual errors (CWRES) plotted against time- and population-predicted concentrations were evaluated. Furthermore, inter individual variability (IIV), parameter precision and shrinkage were taken into account.

#### *Covariate selection, model evaluation and model validation*

For covariate analysis patient characteristics, disease- and treatment-related variables were included (supplementary material, Table S2). The median values for the number of lymphocytes and nucleated cells in the graft were used for missing covariate values. The following covariates were evaluated both on clearance and volume of distribution; baseline lymphocyte count, anti-ATG antibody presence, recipient age, bodyweight, type of conditioning (TBI of Chemo), baseline nucleated cell count in a systemic stepwise forward and backward elimination procedure (with levels of statistical significance respectively set at  $p < 0.05$  and  $p < 0.01$ , corresponding to differences in the OFV of 3.84 and 6.64 (1 degree of freedom)). A covariate effect was included in the final model if the inclusion resulted in a statistically significant and clinically relevant decrease of the random variability of the PK parameter and improved model fit. The final model was evaluated with a prediction-corrected visual predictive check (pcVPC) performed with 500 replicates and further assessed with a non-parametric bootstrap resampling the dataset  $n = 1000$  times. In addition, a normalized prediction distribution of errors (NPDE) was performed, where the prediction differences between the final model and 1000 simulations of the model were evaluated, taking into account the correlation between observations in the same individual and the predictive distribution<sup>8</sup>.

Using the final model, a Shiny application was created based on the Shiny package (version 1.4.0) and the RxODE package in R in order to demonstrate the working of our PK model and to simulate the ATLG exposure for a given patient depending on the dose to be given. A detailed description is shown further on in this supplementary material.

#### *PK exposure metrics*

With the final POPPK model individual parameters of CL, volume of distribution of the central compartment ( $V_1$ ), maximum elimination rate ( $V_{max}$ ), concentration at which the elimination pathway is half saturated ( $K_m$ ), rate of transport from the peripheral compartment to the central compartment ( $K_{21}$ ), maximum rate of transport towards the peripheral compartment ( $T_{max}$ ) and concentration in central volume of distribution at 50% saturation of  $T_{max}$  ( $T_m$ ) were estimated and used to calculate seven different PK exposure metrics (total area under the concentration versus time curve (AUC<sub>tot</sub>), AUC pre-HSCT, AUC post-HSCT, AUC until day 7 post-HSCT, active ATLG concentration at day 0, active ATLG concentration at day 7 and the day that the active ATLG concentration fell below the lympholytic threshold of 1 AU/mL, supplementary material, Table S3).

#### *Clinical outcome parameters and immune recovery*

Clinical endpoints included overall survival, event-free (death, relapse and extensive cGvHD) and relapse-free survival (death and relapse) up to five years post-HSCT, relapse rate, incidence of aGvHD up to 100 days, cGvHD, incidence of viral infections/reactivations up to 100 days and immune cell recovery within the first 3 months post-transplant. Patients lost to follow-up without an event were censored at the last follow-up. For the immune recovery analysis, patients were excluded after they died or relapsed, and cell counts were compared at 4, 8 and 12 weeks after transplantation.

## Supplemental results

### Pharmacokinetic model development and model evaluation

A total of 812 samples from 121 ATLG treated pediatric patients were analysed and used for POPPK model development. The median number of samples per patient was 6, ranging from 3 to 13, with always 1 sample from before the first ATLG dose and multiple samples from s up to 68 days post-transplantation.

ATLG POPPK of this patient group was best described by a two-compartment model with parallel first-order linear and non-linear (Michaelis-Menten) elimination from the central compartment (supplementary Figure S1). In addition, saturable distribution towards the peripheral compartment improved the model fit. This saturable distribution was parameterized as a coefficient of maximum transport rate and the Michaelis–Menten constant. Methods for handling of concentrations below the limit of quantification were extensively evaluated. All options led to the same final structural model, however the most stable model with the most reliable parameter estimates was reached by keeping all the pharmacokinetic data and handling this with a residual error model consisting of a combined proportional and additive error.

The model building process is summarized in the supplementary material Table S4. The base model showed an average clearance of 5.25 L/day with an observed inter-individual variability (IIV) of 75.9% (RSE 7%) and an average central volume of distribution of 28.4 L with an IIV of 59.3% (RSE 6%). After covariate analysis, total bodyweight allometrically scaled was added to clearance and central volume of distribution (supplementary material Figure S2). Bodyweight as covariate was tested in several ways, including bodyweight and age dependent allometry were evaluated. Nevertheless, these more complex allometric covariate relationships did not lead to a significant better model fit in the current dataset.

Diagnostic plots of the final model revealed no major deviations or structural bias (supplementary material Figures S3 and S4). Evaluation of the final model with the bootstrap revealed estimates comparable with the final model PK parameter estimates and their random variability (Table 1). The prediction-corrected VPC confirmed adequate agreement between observed and predicted ATLG concentrations (supplementary material Figure S5 and S6). Also the NPDE results were deemed acceptable. The final model code is provided in the supplementary material. Individual plots per patient with observed and individual model predicted concentration-time curves are shown in this supplementary material.

## Supplemental Tables

Country	Number of patients
Germany	40
Denmark	16
Austria	15
Czech Republic	15
Switzerland	12
Italy	11
Israel	8
Slovakia	4
Total	121

Number of patients	121
<b>Patient age</b> (years), median (range)	9.7 (0.6-18.6)
<b>Graft source</b> , n (overall %)	
Bone marrow	73 (60)
PBSC	29 (24)
Unknown	19 (16)*
<b>Donor type</b> , n (overall %)	
MSD	2 (2)
MUD	101 (83)
Haplo	3 (3)
Unknown	15 (12)*
<b>Conditioning</b> , n (overall %)	
TBI + VP16	53 (44)
Chemo Treosulfan	33 (27)
Chemo Busulfan	17 (14)
Unknown	18 (15)*
<b>Total nucleated cells, 10<sup>8</sup>/kg BW</b> , median (range)	4.75 (0.51-28.7) <sup>a</sup>
<b>Serotherapy ATG dose</b> , mean (range)	
Grafalon, mg/kg BW	42.5 (15-45)
<b>Serotherapy parameters</b> , median (range)	
Start serotherapy, day pre-HSCT	-3 (-11 - -2) <sup>b*</sup>
Days ATG infusion	3 (3-4) <sup>b</sup>
Bodyweight, kg	30.3 (5.6-111.0)
Lymphocytes pre-ATG, 10 <sup>9</sup> /L	0.05 (0.0-9.1) <sup>c</sup>

a) Nucleated cell numbers missing from 30 patients

b) Start day ATLG and days ATG infusion missing from 2 patients

c) Lymphocytes pre-ATG missing from 17 patients

\* If unknown, these patients were not taken into account during covariate analysis

**Table S3. Model estimated pharmacokinetic metrics**

<b>N=121</b>	
Total AUC active ATLG, AU*mL/days (median [IQR])	219.8 [150.2-322.7]
AUC active ATLG pre-HSCT, AU*mL/days (median [IQR])	75.1 [52.9-120.9]
AUC active ATLG post-HSCT, AU*mL/days (median [IQR])	148.8 [90.8-219.8]
AUC active ATLG until day 7 post-HSCT, AU*mL/days (median [IQR])	183.6 [128.7-273.9]
Active ATLG concentration at day 0, AU/mL (median [IQR])	28.8 [20.8-39.2]
Active ATLG concentration at day 7 post-HSCT, AU/mL (median [IQR])	6.8 [4.2-11.1]
The day that active ATLG concentration became <1AU/mL (median [IQR])	15 [12-20]
<b>N=101</b>	
Total AUC active ATLG, AU*mL/days (median [IQR])	233.6 [163.9-354.7]
AUC active ATLG pre-HSCT, AU*mL/days (median [IQR])	75.1 [48.3-121.6]
AUC active ATLG post-HSCT, AU*mL/days (median [IQR])	159.1 [103.4-236.4]
AUC active ATLG until day 7 post-HSCT, AU*mL/days (median [IQR])	192.4 [134.2-282.2]
Active ATLG concentration at day 0, AU/mL (median [IQR])	29.9 [21.2-41.3]
Active ATLG concentration at day 7 post-HSCT, AU/mL (median [IQR])	7.5 [4.4-12.2]
The day that active ATLG concentration became <1AU/mL (median [IQR])	16.0 [13.0-20.0]

<b>Table S4 Model building process</b>						
<b>Model number</b>	<b>Description</b>	<b>Model</b>	<b>Compared against</b>	<b>OFV</b>	<b>ΔOFV</b>	<b>Comment</b>
1	One-compartment with linear elimination	CL = $\Theta 1 \times \text{EXP}(\text{IIV})$ Vd = $\Theta 2 \times \text{EXP}(\text{IIV})$		478.102		
2	One-compartment with parallel linear and non-linear elimination	CL = $\Theta 1 \times \text{EXP}(\text{IIV})$ Vd = $\Theta 2 \times \text{EXP}(\text{IIV})$ Vmax = $\Theta 3 \times \text{EXP}(\text{IIV})$ Km = $\Theta 4 \times \text{EXP}(\text{IIV})$	1	478.102	0	
3	Two-compartment with linear elimination	CL = $\Theta 1 \times \text{EXP}(\text{IIV})$ Vc = $\Theta 2 \times \text{EXP}(\text{IIV})$ Q = $\Theta 3 \times \text{EXP}(\text{IIV})$ Vp = $\Theta 4 \times \text{EXP}(\text{IIV})$	2	178.117	-299.985	
4	Two-compartment with parallel linear and non-linear elimination	CL = $\Theta 1 \times \text{EXP}(\text{IIV})$ Vc = $\Theta 2 \times \text{EXP}(\text{IIV})$ Vp = $\Theta 3 \times \text{EXP}(\text{IIV})$ Q = $\Theta 4 \times \text{EXP}(\text{IIV})$ Vmax = $\Theta 5$ Km = $\Theta 6 \times \text{EXP}(\text{IIV})$	3	57.049	-121.068	
5	Two-compartment with parallel linear and non-linear elimination and saturable distribution	CL = $\Theta 1 \times \text{EXP}(\text{IIV})$ Vd = $\Theta 2 \times \text{EXP}(\text{IIV})$ K21 = $\Theta 3$ Tmax = $\Theta 4$ Tm = $\Theta 5 \times \text{EXP}(\text{IIV})$ Vmax = $\Theta 6$ Km = $\Theta 7 \times \text{EXP}(\text{IIV})$	4	-122.149	-179.198	Base model for covariate analysis Unexplained IIV CL: 75.9% IIV V1: 59.3% IIV Tm: 89.6 % IIV Km: 98.9
6	Two-compartment with parallel linear and non-linear elimination and saturable distribution +	CL = $\Theta 1 \times \text{EXP}(\text{IIV}) \times ((\text{WT}/\text{MWT})^{**} \Theta 10)$	5	-180.562	-58.413	<b>Final model</b> (Bodyweight as predictor (allometrically scaled))

	bodyweight as covariate	$Vd = \Theta 2 \times EXP(IIV) \times ((WT/MWT)** \Theta 11)$				Unexplained
		$K_{21} = \Theta 3$				IIV CL: 58.8%
		$T_{max} = \Theta 4$				IIV V1: 47.1%
		$T_m = \Theta 5 \times EXP(IIV)$				IIV Tm: 78.5%
		$V_{max} = \Theta 6 \times EXP(IIV)$				IIV Vmax: 29.7%
		$K_m = \Theta 7 \times EXP(IIV)$				IIV Km: 78.7%
7	Two-compartment with parallel linear and non-linear elimination and saturable distribution +bodyweight +lymphocyte count at start ATLG as covariate	$CL = \Theta 1 \times EXP(IIV) \times ((WT/MWT)** \Theta 10) \times (1+(LYB/MLYB)*\Theta 12))$	6	-182.544	-1.982	(Bodyweight as predictor (allometrically scaled) and Lymphocytes at start ATLG)
		$Vd = \Theta 2 \times EXP(IIV) \times ((WT/MWT)** \Theta 11)$				Unexplained
		$K_{21} = \Theta 3$				IIV CL: 58.8%
		$T_{max} = \Theta 4$				IIV V1: 47.2%
		$T_m = \Theta 5 \times EXP(IIV)$				IIV Tm: 77.7%
		$V_{max} = \Theta 6 \times EXP(IIV)$				IIV Vmax: 28.6%
		$K_m = \Theta 7 \times EXP(IIV)$				IIV Km: 79.4%
<p>CL=clearance, Vd=volume of distribution, Vc=volume of distribution central compartment, Vp=volume of distribution peripheral compartment, Q= intercompartmental clearance, <math>K_{21}</math>=transfer rate constants connecting compartments, <math>T_{max}</math>=maximum transport rate of distribution towards peripheral compartment, <math>T_m</math>= Michaelis-Menten constant saturable distribution towards peripheral compartment, <math>V_{max}</math>=maximum elimination rate, <math>K_m</math>=concentration at which the elimination pathway is half saturated (Michaelis-Menten Constant), OFV= Objective Function Value, WT= Bodyweight, MWT=Population median bodyweight, LYB= Lymphocyte count at baseline, MLYB= Median Lymphocyte count at baseline. IIV= Inter Individual Variability</p>						

**Table S5 Results of the logistic regression predicting grade II-IV aGvHD and AUC-ROC curves**

Exposure metric	AUC-ROC	Tjur's R <sup>2</sup>
Total AUC active ATLG, AU*mL/days	84.1 (79.4-88.5)	0.258
AUC active ATLG pre-HSCT, AU*mL/days	82.8 (77.2-88.0)	0.204
AUC active ATLG post-HSCT, AU*mL/days	83.7 (79.4-88.0)	0.239
AUC active ATLG until day 7 post-HSCT, AU*mL/days	83.5 (78.4-88.1)	0.234
Active ATLG concentration at day 0, AU/mL	82.6 (79.0-89.1)	0.199
Active ATLG concentration at day 7 post-HSCT, AU/mL	83.9 (79.0-88.2)	0.243
The day that active ATLG concentration became <1AU/mL	84.5 (79.0-88.1)	0.263

The accuracy of the logistic regression models was measured using the AUC-ROC and the .632+bootstrap method<sup>11</sup> and risk regression (v.2021.10.10)<sup>12</sup>

<b>Table S6. Patient characteristics</b>	<b>ATLG low exposure group</b>	<b>ATLG high exposure group</b>
Number of patients	52	49
<b>Sex, n (overall %)</b>		
Male	34 (65)	29 (59)
Female	18 (35)	20 (41)
<b>Patient age (years), median (range)</b>	8.8 (1.1-18.0)	9.4 (0.6-18.6)
0-4, n (overall %)	9 (17)	11 (22)
>4, n (overall %)	43 (83)	38 (78)
<b>Immunophenotype, n (overall %)</b>		
B-cell precursor ALL	43 (83)	34 (69)
T-cell ALL	7 (13)	9 (18)
Other	2 (4)	4 (8)
Unknown	-	2 (4)
<b>Remission status, n (overall %)</b>		
CR1	27 (52)	25 (51)
CR2-3	25 (48)	24 (49)
<b>MRD pre-HSCT, n (overall %)</b>		
Positive	15 (29)	13 (27)
Negative	30 (58)	22 (45)
Unknown	7 (13)	14 (28)
<b>Graft source, n (overall %)</b>		
Bone marrow	34 (65)	40 (82)
PBSC	18 (35)	9 (18)
<b>Donor type, n (overall %)</b>		
MUD	52 (100)	49 (100)
<b>HLA-mismatch, n (overall %)</b>		
10/10	31 (60)	32 (65)
9/10	20 (38)	17 (35)
8/10	1 (1.9)	0 (0)
<b>Conditioning, n (overall %)</b>		
TBI + VP16	36 (69)	16 (33)
Chemo Treosulfan	7 (13)	26 (53)
Chemo Busulfan	9 (17)	7 (14)
<b>GvHD prophylaxis, n (overall %)</b>		
CSA+MTX	45 (87)	43 (88)
CSA+MTX+other	5 (10)	5 (10)
other	2 (4)	1 (2)
<b>Total nucleated cells, 10<sup>8</sup>/kg BW, median (range)</b>	5.40 (0.53-28.7) <sup>a</sup>	4.55 (0.51-23.0) <sup>a3</sup>
Bone marrow	4.81 (0.53-9.7) <sup>a1</sup>	3.80 (0.51-12.55) <sup>a4</sup>
PBSC	11.93 (1.92-28.7) <sup>a2</sup>	11.25 (2.45-23.0) <sup>a5</sup>
<b>CD34+ cells, 10<sup>6</sup>/kg BW, median (range)</b>	5.8 (0.0-33.0) <sup>b</sup>	4.7 (1.5-27.2) <sup>b1</sup>
Bone marrow	5.3 (0.0-12.4) <sup>b</sup>	4.1 (1.5-16.6) <sup>b1</sup>
PBSC	9.4 (2.8-33.0)	8.0 (5.0-27.2)
<b>Serotherapy ATLG dose, mean (range)</b>		
ATLG Grafalon, mg/kg BW	43 (15-45)	45 (31.4-45)
<b>Serotherapy parameters, median (range)</b>		



Start serotherapy, day pre-HSCT	-3 (-5 - -2) <sup>c</sup>	-3 (-5 - -2)
Days ATLG infusion	3 (3-4)	3 (3-4) <sup>d</sup>
Body weight, kg	23.0 (8.4-102.0)	34.0 (5.6-111.0)
Lymphocytes pre-ATLG, 10 <sup>9</sup> /L	0.06 (0.0-1.71) <sup>e</sup>	0.04 (0.0-9.1)

ALL: acute lymphoblastic leukemia; CR: complete remission; MRD: minimal residual disease;

PBSC: peripheral blood stem cell;

MUD: matched unrelated donor; HLA: human leukocyte antigens; BW: body weight; ATLG: anti T-lymphocyte globulin;

TBI: total body irradiation; CSA: cyclosporin A; MTX: methotrexate

a) Nucleated cell numbers missing from 11 patients

a1) Nucleated cell numbers missing from 7 patients

a2) Nucleated cell numbers missing from 4 patients

a3) Nucleated cell numbers missing from 7 patients

a4) Nucleated cell numbers missing from 6 patients

a5) Nucleated cell numbers missing from 1 patients

b) CD34+ numbers missing from 1 patient

b1) CD34+ numbers missing from 2 patients

c) Start day ATLG missing from 1 patient

d) Days ATLG infusion missing from 2 patients

e) Lymphocytes pre-ATLG missing from 3 patients

<b>Table S7. Patient characteristics</b>	<b>ATLG low exposure group</b>	<b>ATLG intermediate exposure group</b>	<b>ATLG high exposure group</b>
Number of patients	43	29	29
<b>Sex, n (overall %)</b>			
Male	29 (67)	18 (62)	16 (55)
Female	14 (33)	11 (38)	13 (45)
<b>Patient age (years), median (range)</b>	8.8 (1.1 - 18.0)	8.3 (0.7-17.7)	9.9 (0.6-18.6)
0-4, n (overall %)	9 (21)	8 (28)	3 (10)
>4, n (overall %)	34 (79)	21 (72)	26 (90)
<b>Immunophenotype, n (overall %)</b>			
B-cell precursor ALL	35 (81)	22 (76)	20 (69)
T-cell ALL	6 (14)	3 (10)	7 (24)
Other	2 (5)	2 (7)	2 (7)
Unknown	-	2 (7)	-
<b>Remission status, n (overall %)</b>			
CR1	24 (56)	13 (45)	15 (52)
CR2-3	19 (44)	16 (55)	14 (48)
<b>MRD pre-HSCT, n (overall %)</b>			
Positive	13 (30)	6 (21)	9 (31)
Negative	24 (56)	15 (52)	13 (45)
Unknown	6 (14)	8 (27)	7 (24)
<b>Graft source, n (overall %)</b>			
Bone marrow	29 (67)	19 (66)	26 (90)
PBSC	14 (33)	10 (34)	3 (10)
<b>Donor type, n (overall %)</b>			
MUD	43 (100)	29 (100)	29 (100)
<b>HLA-mismatch, n (overall %)</b>			
10/10	25 (58)	17 (59)	21 (72)
9/10	17 (40)	12 (41)	8 (28)
8/10	1 (2)	-	-
<b>Conditioning, n (overall %)</b>			
TBI + VP16	30 (70)	13 (45)	9 (31)
Chemo Treosulfan	6 (14)	12 (41)	15 (52)
Chemo Busulfan	7 (16)	4 (14)	5 (17)
<b>GvHD prophylaxis, n (overall %)</b>			
CSA+MTX	37 (86)	26 (90)	25 (86)
CSA+MTX+other	5 (12)	1 (3)	4 (14)
other	1 (2)	2 (7)	-
<b>Total nucleated cells, 10<sup>8</sup>/kg BW, median (range)</b>	5.38 (0.74-28.7) <sup>a</sup>	5.88 (0.53-23.0) <sup>a3</sup>	3.70 (0.51-11.25) <sup>a5</sup>
Bone marrow	4.81 (0.74-9.7) <sup>a1</sup>	4.80 (0.53-12.55) <sup>a4</sup>	3.39 (0.51-6.95) <sup>a5</sup>
PBSC	8.19 (1.92-28.7) <sup>a2</sup>	14.55 (2.45-23.0) <sup>a4</sup>	11.01 (6.03-11.25)
<b>CD34+ cells, 10<sup>6</sup>/kg BW, median (range)</b>	5.8 (0.1-24.0) <sup>b</sup>	5.8 (0.0-33.0)	4.5 (1.5-10.5) <sup>b1</sup>
Bone marrow	5.3 (0.1-12.4) <sup>b</sup>	3.6 (0.0-16.6)	4.3 (1.5-6.1) <sup>b1</sup>

PBSC	9.2 (2.8-24.0)	11.0 (5.0-33.0)	8.1 (8.0-10.5)
<b>Serotherapy ATG dose, mean (range)</b>			
ATLG Grafalon, mg/kg BW	43 (15-45)	45 (45-45)	45 (31.4-45)
<b>Serotherapy parameters, median (range)</b>			
Start serotherapy, day pre-HSCT	-3 (-5 - -2) <sup>c</sup>	-3 (-5 - -2)	-3 (-4 - -3)
Days ATLG infusion	3 (3-4)	3 (3-4)	3 (3-3) <sup>d</sup>
Body weight, kg	29.3 (8.4-102.0)	26.5 (7.8-111.0)	36.3 (5.6-82.0)
Lymphocytes pre-ATLG, 10 <sup>9</sup> /L	0.06 (0.0-1.13) <sup>e</sup>	0.06 (0.0-9.1)	0.04 (0.0-2.1)

ALL: acute lymphoblastic leukemia; CR: complete remission; MRD: minimal residual disease; PBSC: peripheral blood stem cell; MUD: matched unrelated donor;

HLA: human leukocyte antigens; BW: body weight; ATLG: anti T-lymphocyte globulin; TBI: total body irradiation; CSA: cyclosporin A; MTX: methotrexate

a) Nucleated cell numbers missing from 10 patients

a1) Nucleated cell numbers missing from 6 patients

a2) Nucleated cell numbers missing from 4 patients

a3) Nucleated cell numbers missing from 2 patients

a4) Nucleated cell numbers missing from 1 patient

a5) Nucleated cell numbers missing from 6 patients

b) CD34+ cells missing from 1 patient

b1) CD34+ cells missing from 2 patients

c) Start day ATLG missing from 1 patient

d) Days ATLG infusion missing from 2 patients

e) Lymphocytes pre-ATLG missing from 3 patients

**Table S8. Association between patient, disease and transplant characteristics and ATLG exposure**

<b>Characteristic</b>	<b>low ATLG exposure n=52</b>	<b>high ATLG exposure n=49</b>	<b>p-value</b>
<b>Patient age (years), median (IQ-range)</b>	8.8 (5.8-13.5)	9.4 (6.2, 14.6)	>0.9
0-4, n (overall %)	9 (17)	11 (22)	0.5
<b>Remission status, n (overall %)</b>			>0.9
CR1	27 (52)	25 (51)	
CR2-3	25 (48)	24 (49)	
<b>Minimal Residual Disease status, n (overall %)</b>			0.7
Negative	30 (67)	22 (63)	
Positive	15 (33)	13 (37)	
Unknown	7	14	
<b>HLA match, n (overall %)</b>			0.8
HLA (10/10)	31 (60)	32 (65)	
HLA (9/10)	20 (38)	17 (35)	
HLA (8/10)	1 (1.9)	0 (0)	
<b>Conditioning, n (overall %)</b>			<0.001
TBI + VP16	36 (69)	16 (33)	
Chemo Treosulfan	7 (13)	26 (53)	
Chemo Busulfan	9 (17)	7 (14)	
<b>Graft source, n (overall %)</b>			0.07
Bone marrow	34 (65)	40 (82)	
PBSC	18 (35)	9 (18)	

**Table S9. Results of the multivariate analyses of aGvHD and relapse rate**

<b>aGvHD</b>	<b>Subdistribution hazard ratio (95% CI)</b>	<b>p value</b>
<i>ATLG exposure</i>		
Low-exposure	1.00 (ref)	
High-exposure	0.10 (0.03-0.31)	<0.001
<i>Conditioning regimen</i>		
Chemotherapy	1.00 (ref)	
TBI	0.55 (0.26-1.17)	0.12
<i>Complete remission state</i>		
CR 1	1.00 (ref)	
CR 2-3	0.68 (0.33 - 1.40)	0.3
<i>Age</i>		
>4 years of age	1.00 (ref)	
<4 years of age	1.06 (0.39-2.88)	>0.9
<i>Stem cell source</i>		
Bone marrow	1.00 (ref)	
Peripheral blood stem cells	1.35 (0.61 – 2.95)	0.5
<b>Relapse rate</b>		
<i>ATLG exposure</i>		
Low-exposure	1.00 (ref)	
High-exposure	2.41 (0.92-6.36)	0.075
<i>Conditioning regimen</i>		
Chemotherapy	1.00 (ref)	
TBI	0.64 (0.23-1.80)	0.4
<i>Complete remission state</i>		
CR 1	1.00 (ref)	
CR 2-3	2.64 (1.09-7.01)	0.031
<i>Age</i>		
>4 years of age	1.00 (ref)	
<4 years of age	2.40 (0.88-6.50)	0.11
<i>Stem cell source</i>		
Bone marrow	1.00 (ref)	
Peripheral blood stem cells	2.39 (0.88 – 6.50)	0.088

ATLG: anti T-lymphocyte globulin, CR: complete remission, TBI: total body irradiation

**Table S10. Bivariate analysis of graft source and ATLG exposure on relapse rate and death**

Characteristic	total number of events	1 year post-HSCT	2 years post-HSCT	p-value
<b>Relapse</b>	25			0.002
low exposure ATLG + BM		8.8% (2.2-21%)	17% (5.8-32%)	
high exposure ATLG + BM		18% (8-32%)	27% (14-42%)	
low exposure ATLG + PBSC		13% (1.9-34%)	13% (1.9-34%)	
high exposure ATLG + PBSC		60% (17-86%)	60% (17-86%)	
<b>Death</b>	4			0.3
low exposure ATLG + BM		0%	0%	
high exposure ATLG + BM		2.5% (0.19-11%)	2.5% (0.19-11%)	
low exposure ATLG + PBSC		12% (1.8-32%)	12% (1.8-32%)	
high exposure ATLG + PBSC		0%	0%	

**Table S11. Bivariate analysis of TBI and ATLG exposure on relapse rate**

Characteristic	total number of events	1 year post-HSCT	2 years post-HSCT	p-value
<b>Relapse</b>	25			0.083
low exposure ATLG + chemo		26% (7.6-50%)	26% (7.6-50%)	
high exposure ATLG + chemo		31% (16-47%)	38% (21-55%)	
low exposure ATLG + TBI		2.9% (0.21-13%)	11 (2.5-25%)	
high exposure ATLG + TBI		14% (2.0-37%)	22% (4.8-46%)	
<b>Death</b>	4			0.7
low exposure ATLG + chemo		0.00%	0.00%	
high exposure ATLG + chemo		3.0% (0.22-14%)	3.0% (0.22-14%)	
low exposure ATLG + TBI		5.6% (0.98-17%)	5.6% (0.98-17%)	
high exposure ATLG + TBI		0.00%	0.00%	

**Table S12. Co-occurrence of relapse and mortality**

	High ATLG exposure + CR1	High ATLG exposure + CR2/3	Low ATLG exposure + CR1	Low ATLG exposure + CR2/3
Censored	20	11	22	19
Death after relapse	1	4	1	3
Death without relapse	0	1	1	2
Relapse without death	4	8	3	1

## Supplemental Figures

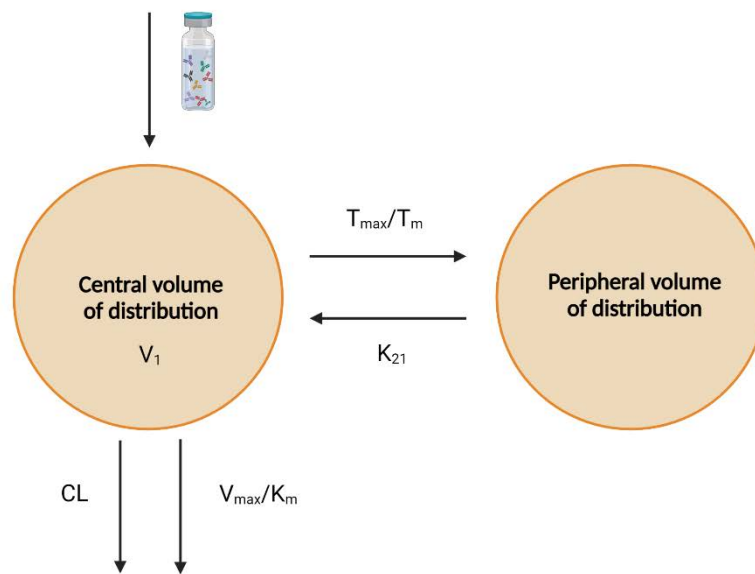


**Figure S1. Final pharmacokinetic model structure.** A two-compartmental model with parallel linear and non-linear clearance best described the ATLG concentration-time data. Bodyweight, allometrically scaled, was added as covariate since it significantly explained ATLG PK variability. CL: clearance;  $K_m$ : Michaelis Menten constant of non-linear elimination;  $K_{21}$ : distribution constant towards the central compartment;  $T_m$ : Michaelis Menten constant of non-linear distribution;  $T_{\max}$ : maximum rate of non-linear distribution;  $V_{\max}$ : maximum rate of non-linear elimination.

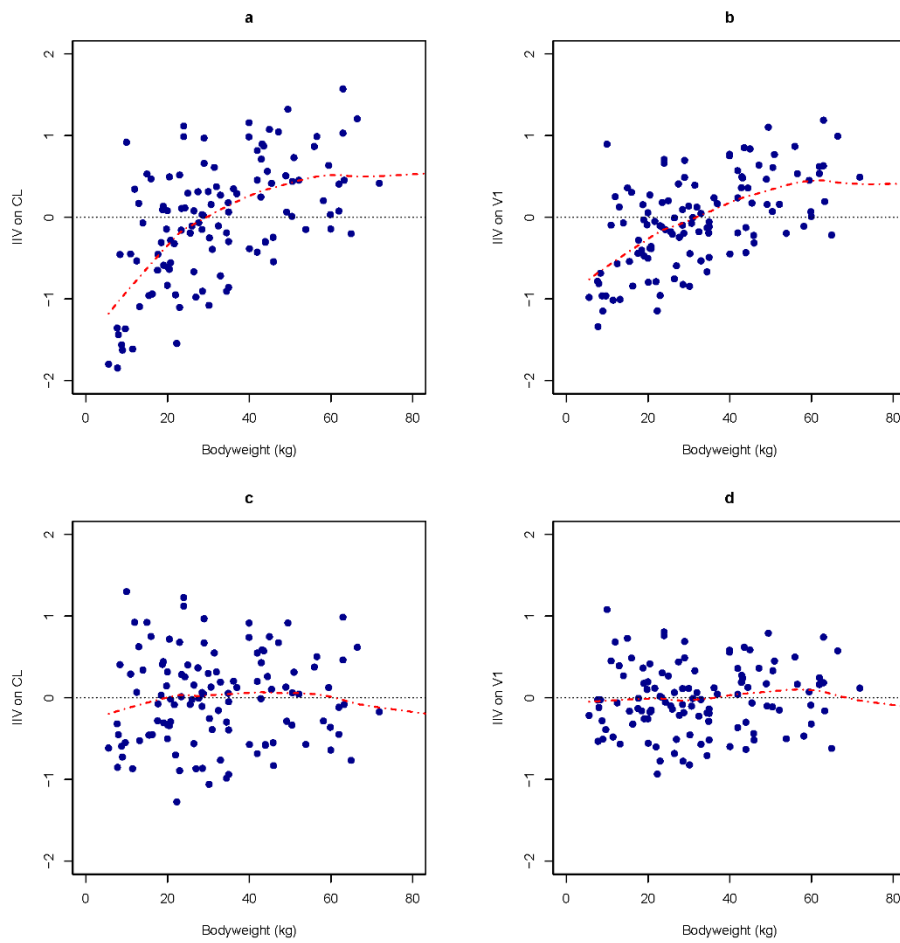


**Figure S2. Impact of bodyweight as covariate on inter-individual variability of ATLG clearance and central volume of distribution before (a,b) and after (c,d) model inclusion. A, B)** Bodyweight had a significant positive correlation with the interindividual variability of ATLG clearance (IIV on CL) and central volume of distribution (IIV on V1) as shown by the locally weighted smoothing (LOESS) regression line (red). **C, D)** Inclusion of total bodyweight allometrically scaled as predictor of IIV on CL and V1 to the model, markedly reduced the impact of bodyweight on IIV on V1 and CL as shown by the LOESS regression line.



### Goodness of fit final model

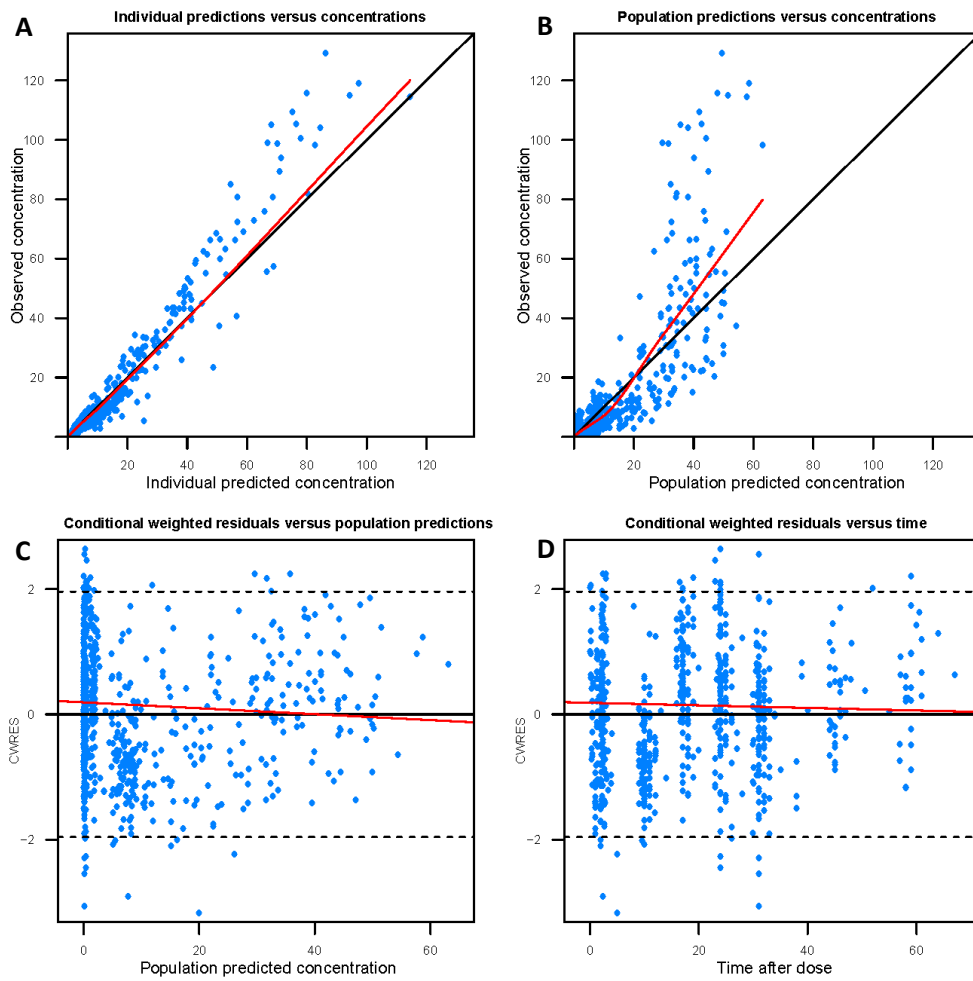


**Figure S3 Goodness of fit plots for the final PK model.** **A)** Individual predicted concentrations vs. observed concentrations (linear scale). **B)** Populations predicted concentrations vs. observed concentrations (linear scale). **C)** Conditional weighted residuals vs. population prediction (linear scale). **D)** Conditional weighted residuals vs. time after dose (linear scale). The red line represents the local regression line. The solid black line represents the linear regression line with as slope = 1 (panel A, B) or define zero (panel C, D). The black dotted lines represent  $\pm 1.96$ , the 2.5% and 97.5% quantiles for normal distribution (panel C, D).

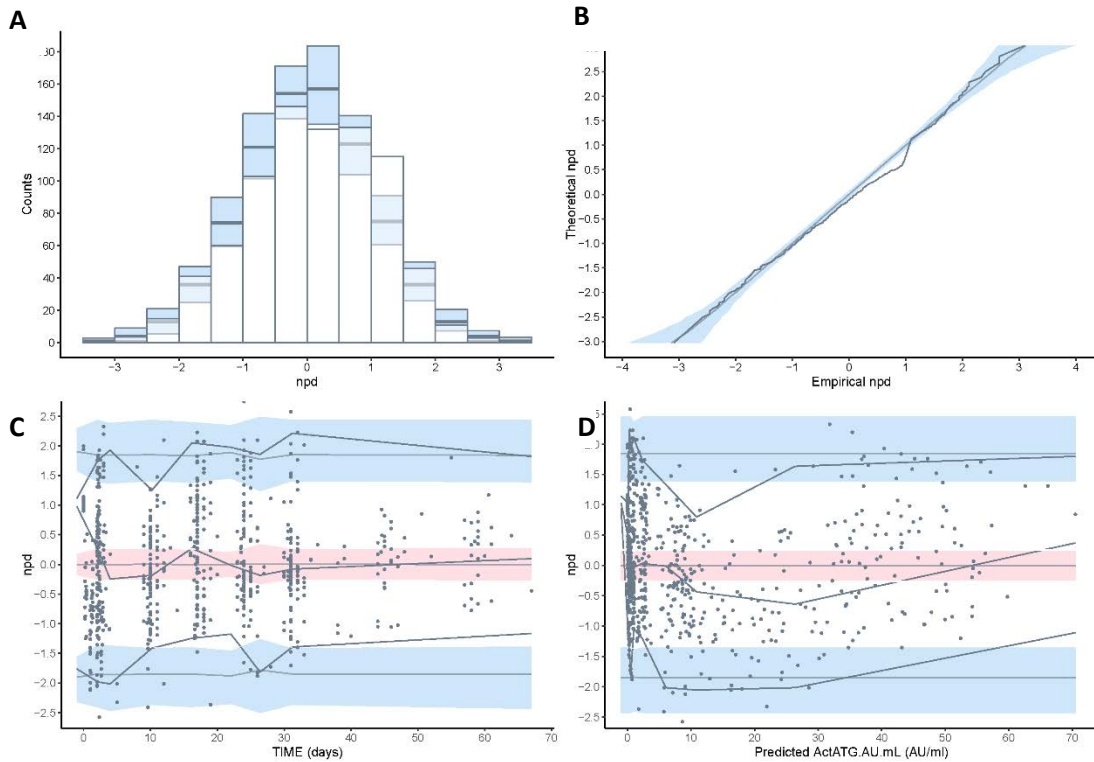


**Figure S4 Normalized Prediction Distribution Errors (NPDE) plots.** **A)** Histogram of the distribution of the NPDE of the final model. **B)** QQ-plot of the distribution of the NPDE vs. the theoretical  $N(0, 1)$  distribution. **C)** NPDE vs. time. **D)** NPDE vs. the predicted active ATLG concentration in AU/mL. Prediction intervals are plotted as a colored area (blue for the 2.5 and 97.5th percentiles and pink for the median).

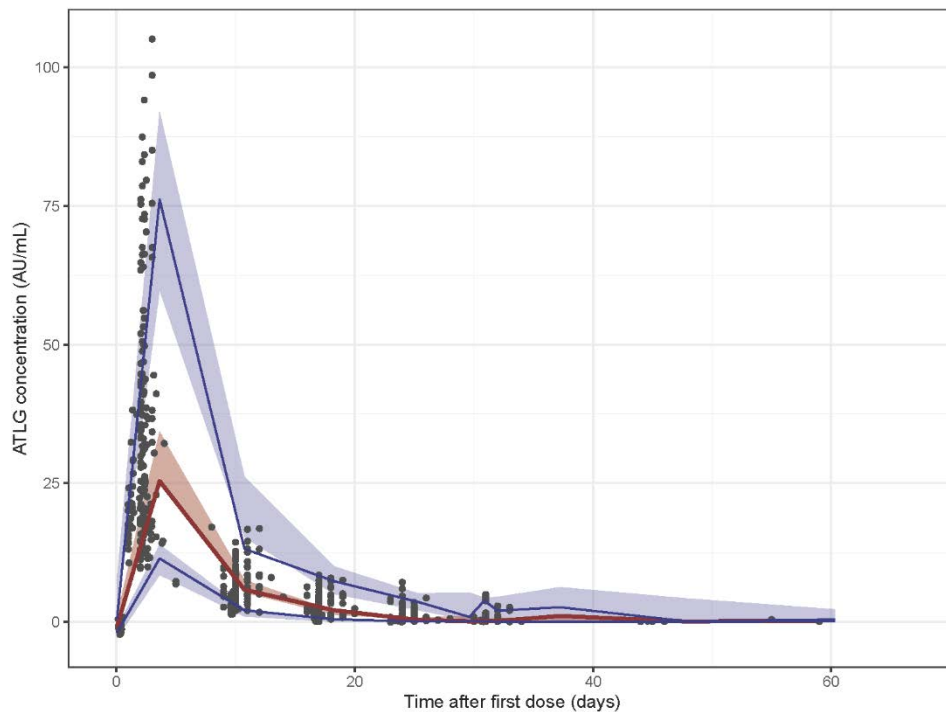


**Figure S5 Prediction corrected visual predictive check of the final pharmacokinetic model on normal scale.** Comparisons were performed between the 50th (red solid line), the 10th, and the 90th (blue solid) percentiles of the observed active ATLG plasma concentrations (closed circles) vs. time after first dose (days) and the 80% confidence interval (shaded area) obtained from 500 simulations

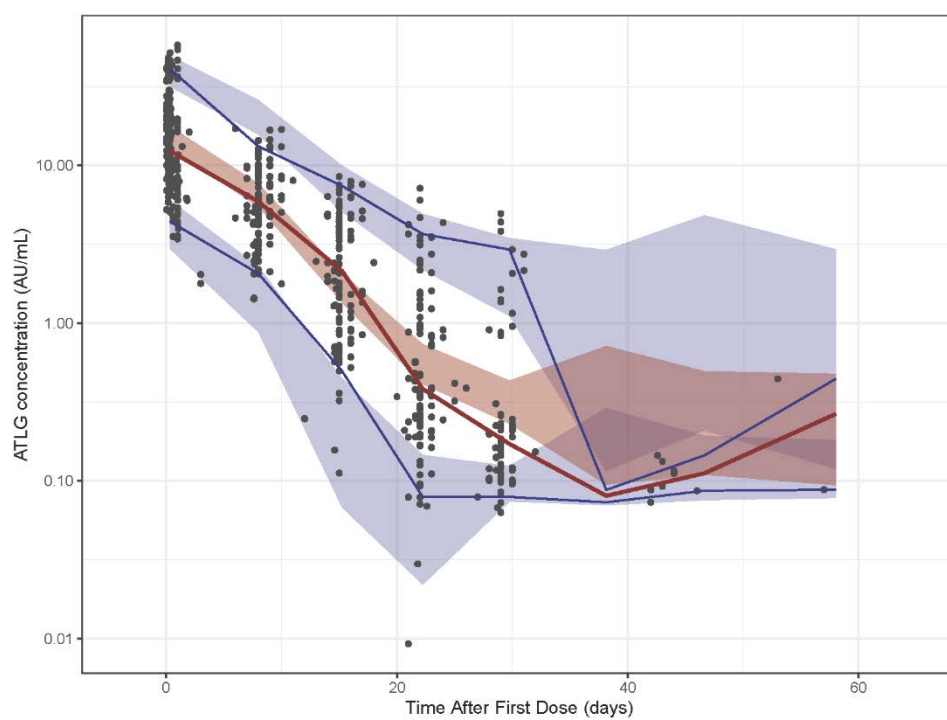


**Figure S6 Prediction corrected visual predictive check of the final pharmacokinetic model on lognormal scale.** Comparisons were performed between the 50th (red solid line), the 10th, and the 90th (blue solid) percentiles of the observed active ATLG plasma concentrations (closed circles) vs. time after dose (days) and the 80% confidence interval (shaded area) obtained from 500 simulations.

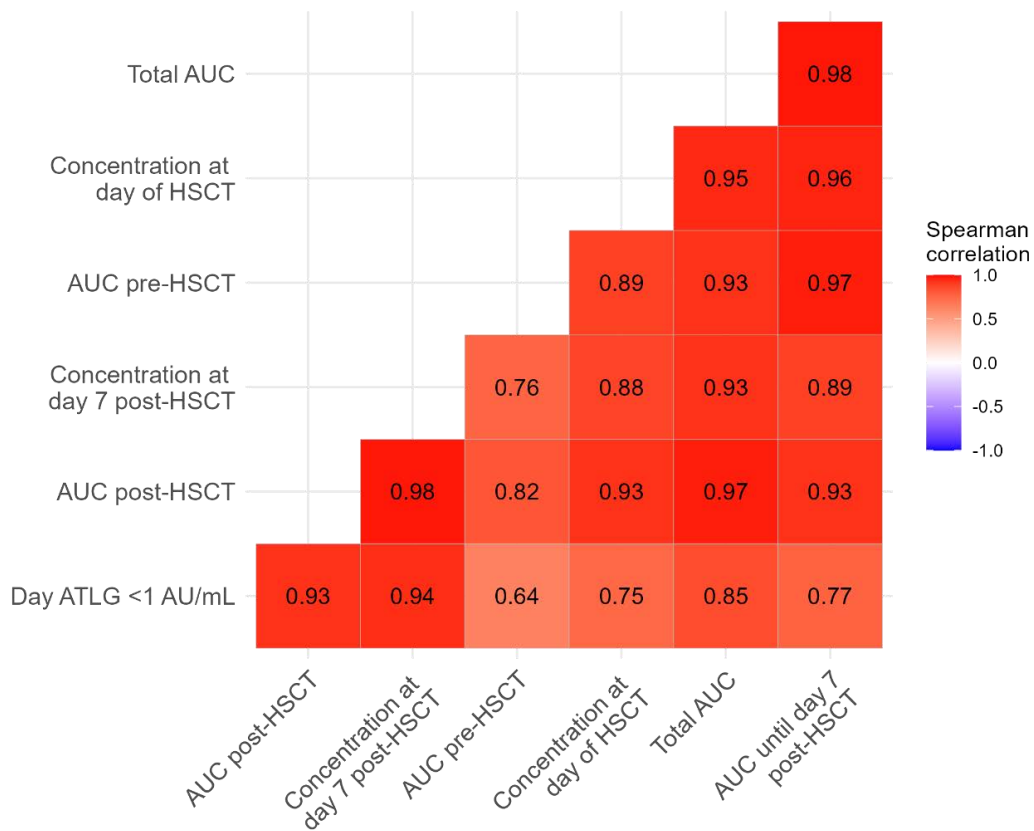


**Figure S7 Correlation plot of the ATLG exposure metrics.** All ATLG exposure metrics correlated well with each other. The day active ATLG <1 AU/mL correlated best with active ATLG AUC post-HSCT and the active ATLG concentration at day 7 after transplantation. The weakest correlation was found between the day active ATLG <1 AU/mL and the AUC pre-HSCT.

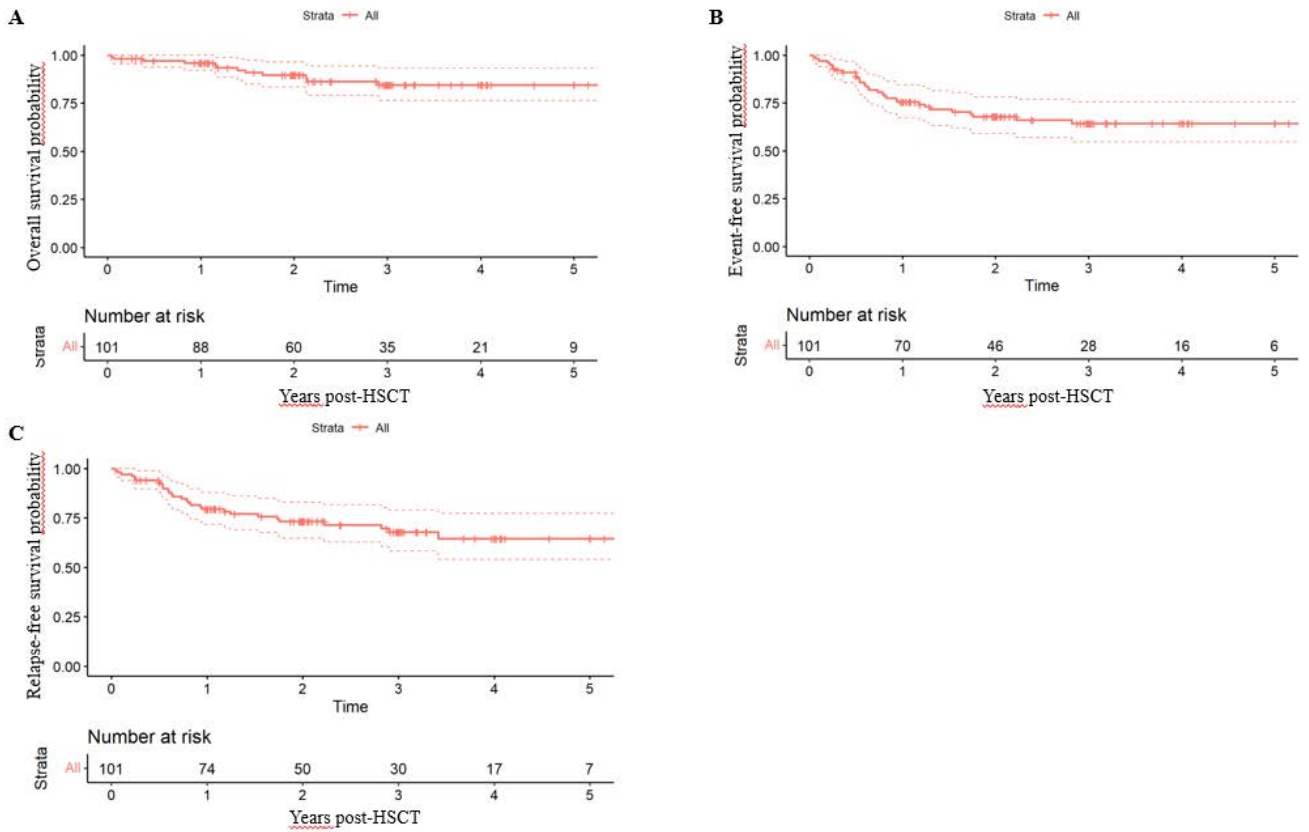


**Figure S8 Kaplan-meier curves for overall, event-free and relapse-free survival. A)** Overall survival in the total cohort was high with a two year survival probability of 90%. **B)** Event-free survival (taking into account death, relapse and extensive cGvHD) was 75% and 68% at one and two years post-HSCT and 64% at five years post-HSCT. **C)** Relapse-free survival at one year after transplantation was 79%, decreasing to 73% and 65% at respectively two and five years post-transplantation.

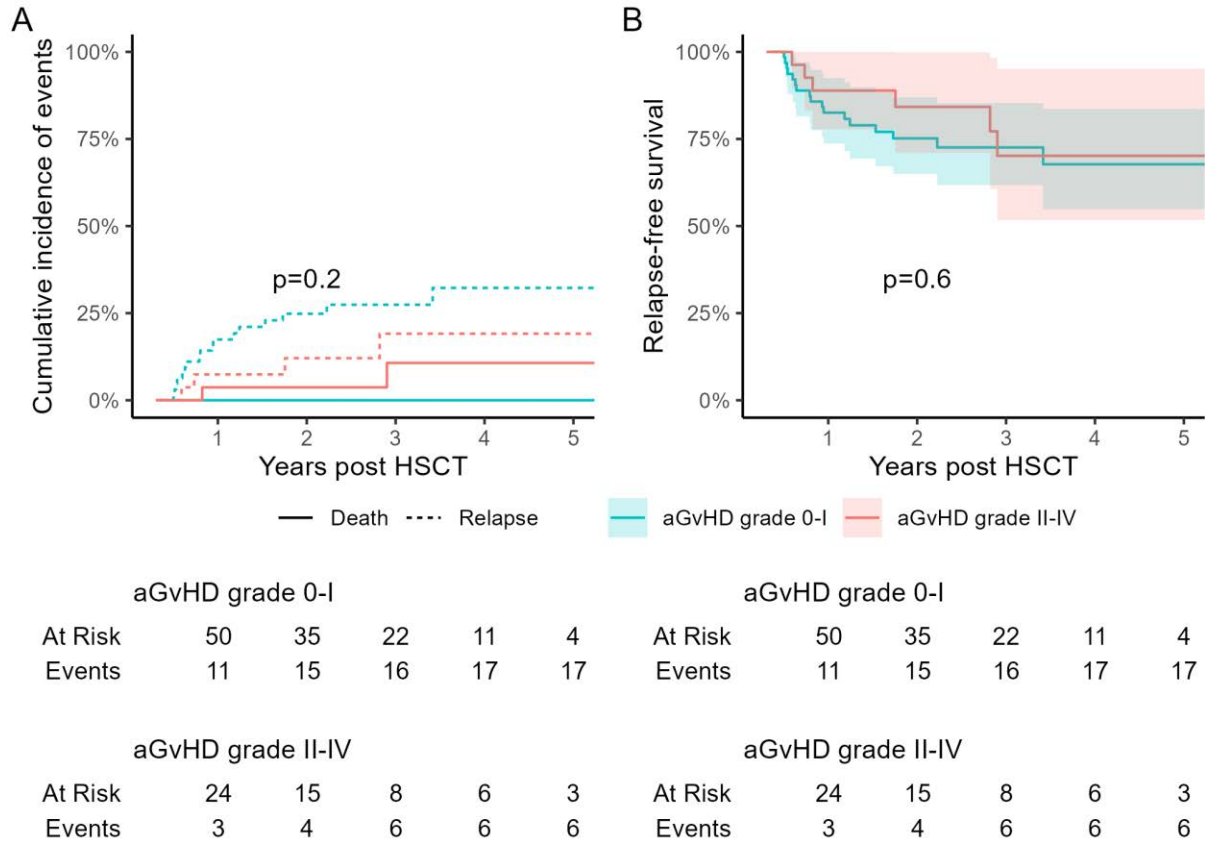


**Figure S9 Relapse and relapse-free survival in patients with or without aGvHD. A)** In patients without aGvHD or grade I aGvHD (blue) the incidence of relapse was higher compared to patients with aGvHD grade II-IV (red), however this was not significant ( $p=0.2$ ). **B)** Relapse-free survival probability was not different between patients with or without aGvHD ( $p=0.6$ ).

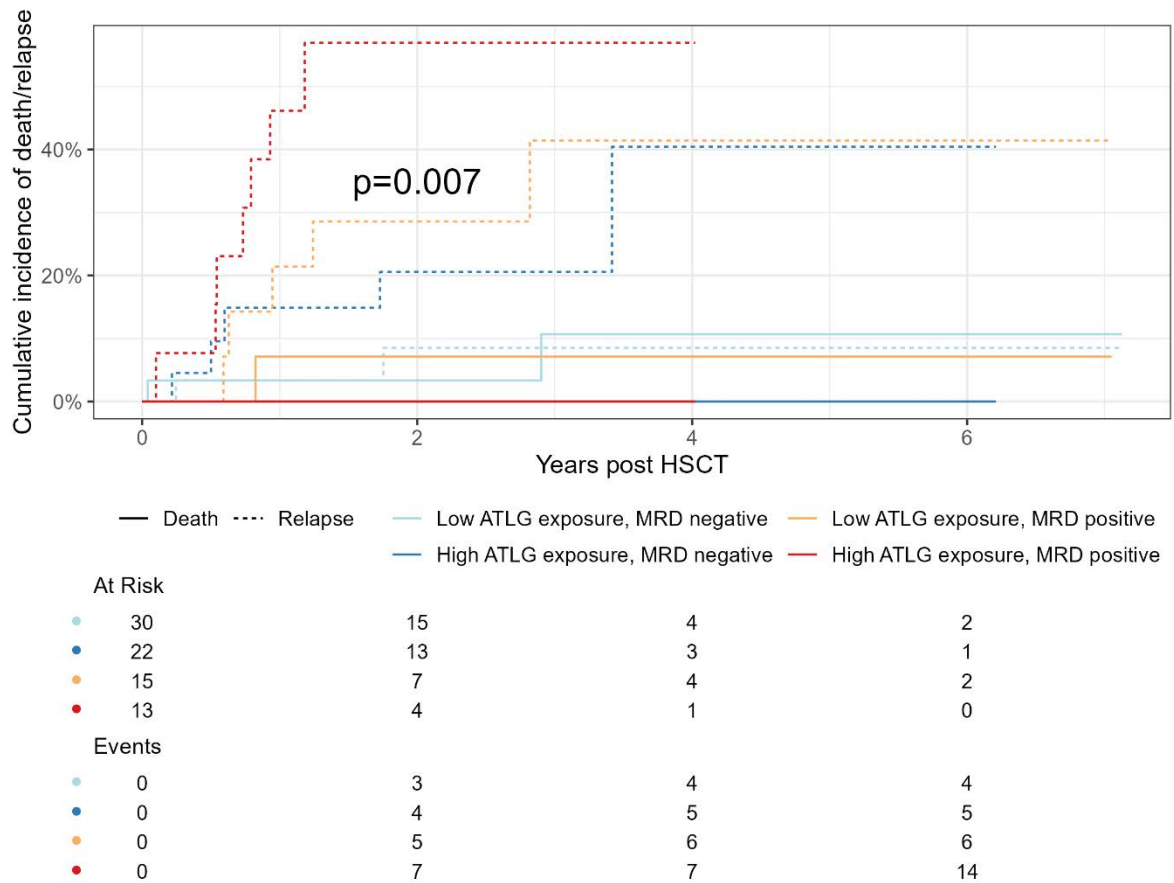
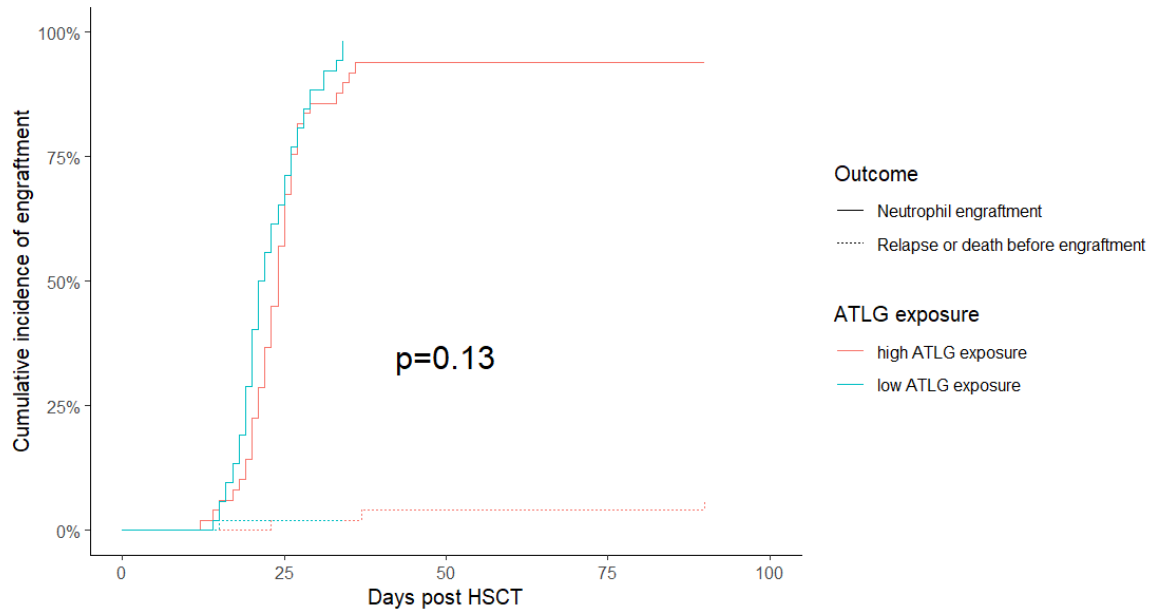


**Figure S10 Effect of ATLG exposure on relapse-rate in MRD positive vs. negative patients** MRD positive patients had a higher risk for relapse with 57% 2 year relapse-rate in high ATLG exposure patients (red dotted line) and 29% in low ATLG exposure patients (yellow dotted line) vs. respectively 21% and 9% in high (dark blue dotted line) and low ATLG (light blue dotted line) exposed MRD negative patients (p=0.007). Cumulative incidence of death was not significantly different between these four groups (solid lines). Of 21 patients data on MRD state was missing.



	high ATLG exposure				
At Risk	49	20	1	1	0
Events	0	34	48	48	49
	low ATLG exposure				
At Risk	52	17	0	0	0
Events	0	38	52	52	52

**Figure S11 Effect of ATLG exposure on engraftment.** Cumulative incidence of engraftment was not significantly different between the ATLG low (blue solid line) and high exposure group (red solid line) ( $p=0.13$ ). One patient in the low ATLG exposure group (dotted blue line) and three patients in the high ATLG exposure group (red dotted line) relapsed or died before engraftment.



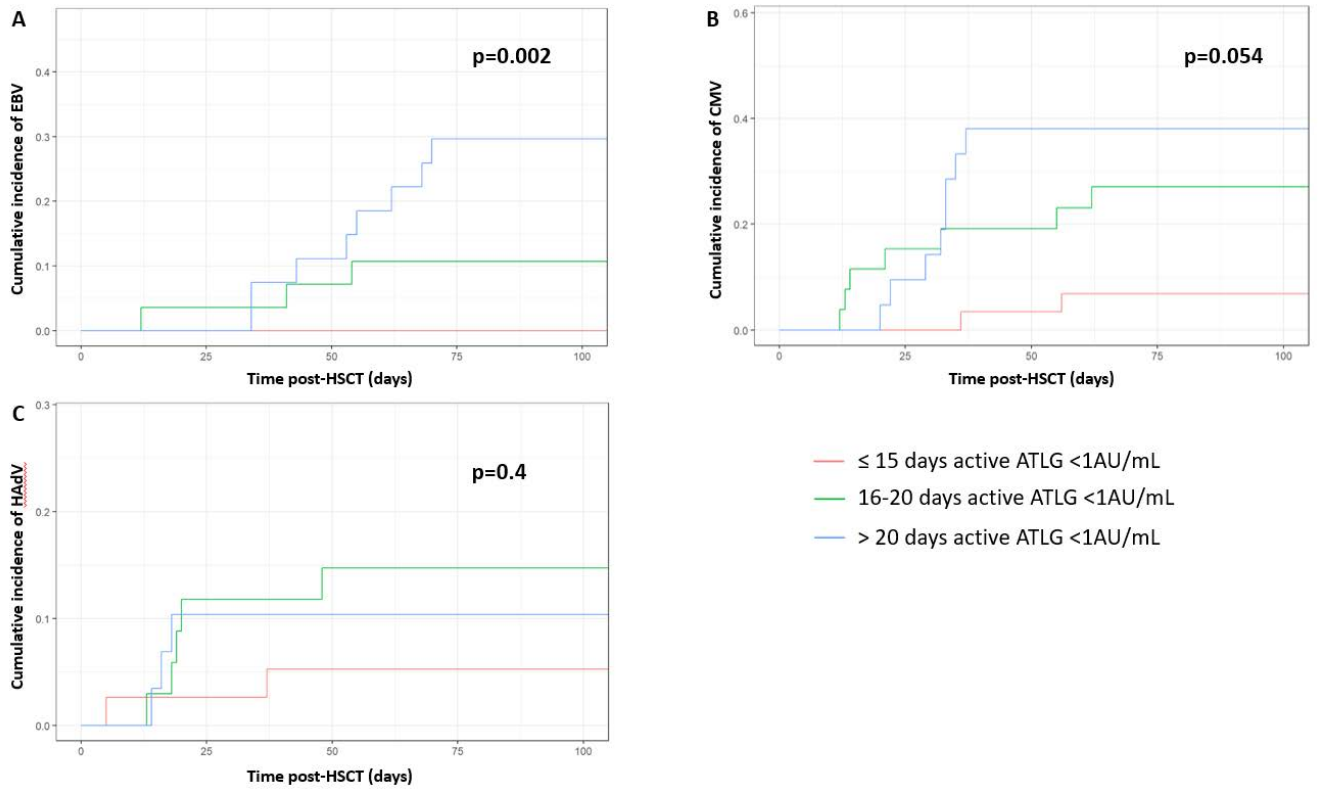


**Figure S12 Competing risk cumulative incidence curves for EBV, CMV and HadV** **A)** The incidence of EBV infection/reactivation was higher in patients with longer ATLG exposure after transplantation compared to patient that cleared their ATLG faster (Gray's test analysis cumulative incidence EBV at 100 days post-HSCT, low ATLG exposure group 0% vs. intermediate ATLG exposure group 11% vs. high ATLG exposure group 30%,  $p=0.002$ ).  $N = 90$  (patients at risk). **B)** Cumulative incidence CMV at 100 days post-HSCT, low ATLG exposure group 6.9% vs. intermediate ATLG exposure group 27% vs. high ATLG exposure group 38%,  $p=0.054$ , 76 patients at risk. **C)** Ten patients were diagnosed with an HAdV infection and there was no correlation with ATLG exposure ( $p=0.4$ ).

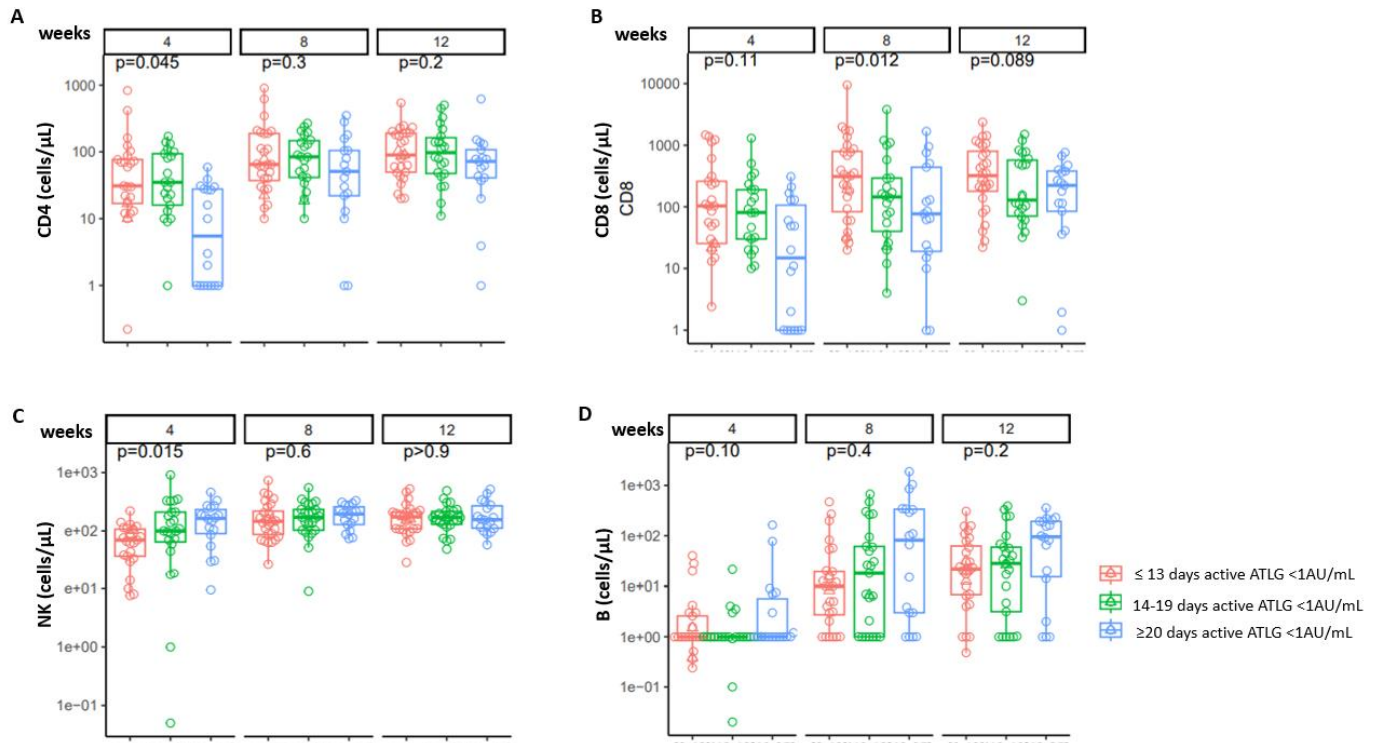


**Figure S13 Immune reconstitution at 4, 8 and 12 weeks post-HSCT** **A)** CD4 T-cell reconstitution was delayed in patients with the longest active ATL exposure ( $>20$  days post-HSCT, median CD4 cells/ $\mu$ L at 4 weeks 30.0 vs. 24.0 vs. 3.0;  $p=0.045$ ). After 8 weeks post-transplantation no difference in CD4 T-cells numbers was seen between the three groups. **B)** CD8 T-cell recovery is faster in patients with a low or short active ATL exposure at least up to 12 weeks after transplantation compared to patients with longer exposure (median CD8 cells at 8 weeks post-HSCT 310.8 vs. 115.0 vs. 65.0 cells/ $\mu$ L;  $p=0.012$ ). **C)** NK-cells recovered faster in patients in the high exposure group, with a significant difference at 4 weeks post-transplantation (NK-cell numbers median 64.4 vs. 99.2 vs. 160.0 cells/ $\mu$ L;  $p=0.015$ ). **D)** There was no effect of ATL exposure on B-cell recovery after transplantation. For CD4 and CD8 reconstitution week 4  $n=72$  of which 10 are estimated, week 8  $n=72$  of which 8 are estimated, week 12  $n=71$  of which 8 are estimated. For NK and B cell recovery week 4  $n=72$  of which 8 are estimated, week 8  $n=72$  of which 4 are estimated, week 12  $n=71$  of which 4 are estimated

**List of participating institutions**

<b>Country</b>	<b>Institution</b>	<b>Responsible physician</b>
Austria	Vienna - St. Anna Kinderspital	Christina Peters, Herbert Pichler, Anita Lawitschka, Natascha Zubrovskaya, Wolfgang Holter
Czech Republic	Prague - Hospital Motol, Charles University Motol Prague	Petr Sedlacek
Denmark	Copenhagen - Rigshospitalet	Marianne Ifversen, Carsten Heilmann
Germany	Bonn - Universitätsklinikum Bonn	Dagmar Dillo, Cathy Scholtes
	Düsseldorf - Universitätsklinikum Düsseldorf	Roland Meisel, Friedhelm Schuster
	Essen - Universitätsklinikum Essen	Oliver Basu, Dirk Reinhardt
	Frankfurt - Klinik für Kinderheilkunde III University Hospital Frankfurt	Peter Bader, Jan Sörensen, Andrea Jarisch
	Hannover - Med. Hochschule Hannover	Martin Sauer, Britta Maecker-Kohlhoff
	Leipzig - Uniklinik, Universitätsmedizin Leipzig	Holger Christiansen, Sven Kühl
	München - Klinikum der Universität München	Michael Albert, Tobias Feuchtinger
	Münster - Universitätsklinikum Münster	Claudia Rössig, Birgit Burkhardt
	Regensburg - Universitätsklinikum Regensburg	Selim Corbacioglu, Jürgen Föll
	Ulm - Universitätskinderklinik Ulm	Ansgar Schulz, Manfred Hönig
	Würzburg - Universitätskinderklinik Würzburg	Paul Schlegel, Matthias Eyrich
Israel	Haifa - Rambam Medical Center	Irina Zaidman
	Petach-Tikva - Schneider Children's Medical Center of Israel	Jerry Stein
Italy	Monza - Clinica Pediatrica Università degli Studi di Milano Bicocca, Fondazione MBBM/ASST Monza, Ospedale San Gerardo	Adriana Balduzzi
Slowakia	Bratislava - Pediatric University Teaching Hospital	Peter Svec, Sabina Sufliarska, Julia Horakova

Switzerland

Basel - Universitäts-Kinderspital beider Basel	Nicolas van der Weid
Geneva - HUG Hôpitaux Universitaire de Genève	Marc Ansari
Zürich - Universitäts-Kinderspital Zürich	Tayfun Güngör, Ulrike Zeilhofer, Jean Pierre Bourquin, Federica Achini

## Final population PK model code

\$PROBLEM PK

\$INPUT ID TIME DV TADD ATGnr dag\_na SCT AMT RATE2 RATE MDV EVID WT LyDayPreStartATG  
LYMFpreATG CENTRE T\_G ATGtotal DaysATG DoseMgKgDay DayATGStart RecipientAge DICODE  
GRAFT ADA ADAOVERALL TIMEDOS TLASTDOSE NucleatedCells Type COND1 COND2  
codeDayATGStart

\$DATA ActATGGrafalonforummd4n.csv ;

IGNORE=C

\$SUBROUTINES ADVAN6 TOL=9

\$MODEL

NCOMP=3

COMP=(CENTRAL DEFOBS DEFDOSE)

COMP=(PERIPH)

COMP= AUC

\$PK

IF(NEWIND.LT.2) THEN

IFL = 0

TAD = 0

ENDIF

IF(EVID.EQ.1.OR.EVID.EQ.4) THEN

TDOS = TIME

TAD = 0

IFL = 1

ENDIF

IF(IFL.EQ.1.AND.EVID.NE.1.AND.EVID.NE.4)TAD=TIME-TDOS

MWT=WT/30.3 ;Typical Weight

TVCL = THETA(1) \* (MWT\*\*THETA(10)); \* (1+MLYM\*THETA(10))

CL = TVCL \* EXP(ETA(1))

;Central volume of distribution

TVV1 = THETA(2) \* (MWT\*\*THETA(11))

V1 = TVV1 \* EXP(ETA(2))

;Distribution

TVK21 = THETA(3)

K21 = TVK21

TVTMAX= THETA(4)

TMAX = TVTMAX

TVTM = THETA(5)

TM = TVTM \* EXP(ETA(3))

;Non-linear clearance

TVVMAX= THETA(6)

VMAX = TVVMAX \* EXP(ETA(4))

TVKM = THETA(7)

KM = TVKM \* EXP(ETA(5))

K = CL/V1

S1 = V1

\$DES

C1 = A(1)/V1

DADT(1)= -K\*A(1)-(VMAX\*C1)/(KM+C1)-(TMAX\*C1)/(TM+C1)+K21\*A(2)

DADT(2)= (TMAX\*C1)/(TM+C1)-K21\*A(2)

DADT(3)=C1

\$ERROR

IPRED = F

W = SQRT(THETA(8)\*\*2\*IPRED\*\*2 + THETA(9)\*\*2)

Y = IPRED + W\*ERR(1)

IRES = DV-IPRED

IWRES = IRES/w

AUC=A(3)

\$THETA

(0, 5.26) ; CL

(0, 28.9) ; V1

(0, 0.0459) ; K21

(0, 1790) ; Tmax

(0, 3540) ; Tm

(0, 3.95) ; Vmax

(0, 0.261) ; Km  
(0,0.324) ; error prop  
(0,0.0098) ; error add  
(0,0.788) ; EXP CL  
(0,0.583) ; EXP V

\$OMEGA BLOCK(2)

0.783 ;CL

0.27 0.339 ;V1

\$OMEGA

1.13 ;Tm

0.512 ;Vmax

3.06 ;Km

\$SIGMA

1 FIX ;

\$EST METHOD=1 INTER MAXEVAL=9999 NOABORT SIG=2 SIGL=6 PRINT=5 POSTHOC

\$COV

; Xpose

\$TABLE ID TIME TAD DV MDV EVID AMT AUC IPRED PRED IWRES ETA1 ETA2 ETA3 ETA4 CL V1  
CWRES WT LyDayPreStartATG LYMFpreATG CENTRE T\_G ATGtotal DaysATG DoseMgKgDay  
DayATGStart RecipientAge DICODE GRAFT ADA ADAOVERALL TIMEDOS TLASTDOSE NucleatedCells  
Type COND1 COND2 codeDayATGStart ONEHEADER NOPRINT FILE=sdtabSTEP7

\$TABLE ID TIME TAD CL V1 DV KM ATGNR AMT RATE MDV EVID ONEHEADER NOPRINT  
FIRSTONLY FILE=patabSTEP7

## Shiny ATLG Population PK model simulation application

Using the final ATLG model, a Shiny application was created based on the Shiny package (version 1.4.0) and the RxODE package in R in order to demonstrate the working of our population PK model and to simulate the ATLG exposure for a given patient depending on the dose to be given. The R script can be found through: <https://zenodo.org/records/7944182>

Patient weight, number of ATLG doses, (to be given) cumulative dose in mg/kg, infusion time in hours and time between the first ATLG dose and the day of HSCT in days were in the input panel. The expected day (after HSCT) that active ATLG concentration will be 1 AU/mL (red dotted line), the 90% prediction interval and the 50th percentile of the concentration predictions were plotted in the output figure. Screen shots of the developed shiny app are shown below. Panel A shows the result of a patient with 10 kg bodyweight, receiving a cumulative dose of 15 mg/kg ATLG divided over 3 dosages of 5 mg/kg, starting at day -3 before HSCT. Based on the model the predicted day that the active ATLG concentration <1 AU/mL is day 7 post-HSCT with a 90% prediction interval between 2.5 and 15 days post-HSCT. Panel B shows the result of a patient with 10 kg bodyweight, receiving a cumulative dose of 45 mg/kg ATLG divided over 3 dosages of 15 mg/kg, starting at day -3 before HSCT. Based on the model the predicted day that the active ATLG concentration <1 AU/mL is day 17 post-HSCT. Panel C shows the result of a patient with 60 kg bodyweight, receiving a cumulative dose of 15 mg/kg ATLG divided over 3 dosages of 5 mg/kg, starting at day -3 before HSCT. Based on the model the predicted day that the active ATLG concentration <1 AU/mL is day 12 post-HSCT. Panel D shows the result of a patient with 60 kg bodyweight, receiving a cumulative dose of 45 mg/kg ATLG divided over 3 dosages of 15 mg/kg, starting at day -3 before HSCT. Based on the model the predicted day that the active ATLG concentration <1 AU/mL is day 20 post-HSCT.

### A ATLG Population PK Model Simulation

Patient characteristics:

Weight of patient (kg)

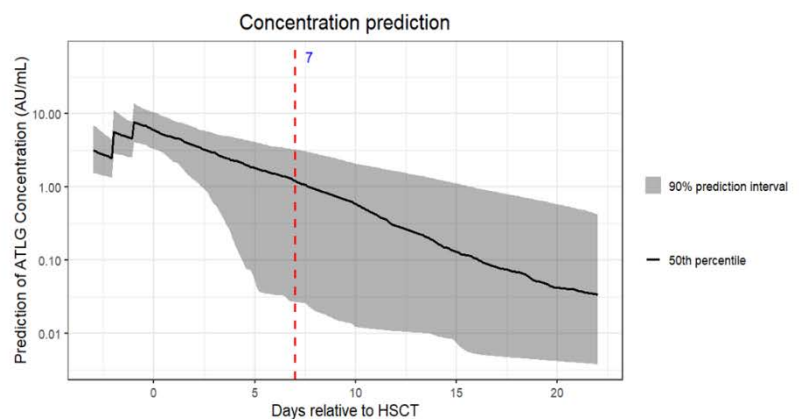
Number of doses (times)

Cumulative dose (mg/kg)

Infusion hours (hrs)

Time between first infusion and HSCT (days)

Plot in log scale  
 Yes  
 No





## B ATLG Population PK Model Simulation

Patient characteristics:

Weight of patient (kg)

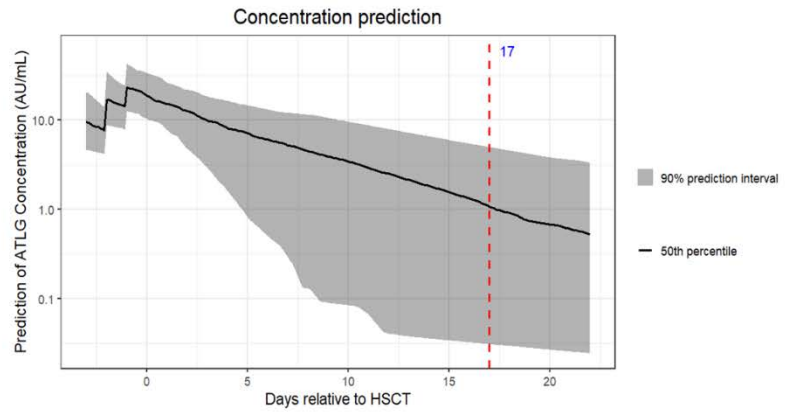
Number of doses (times)

Cumulative dose (mg/kg)

Infusion hours (hrs)

Time between first infusion and HSCT (days)

Plot in log scale  
 Yes  
 No



## C ATLG Population PK Model Simulation

Patient characteristics:

Weight of patient (kg)

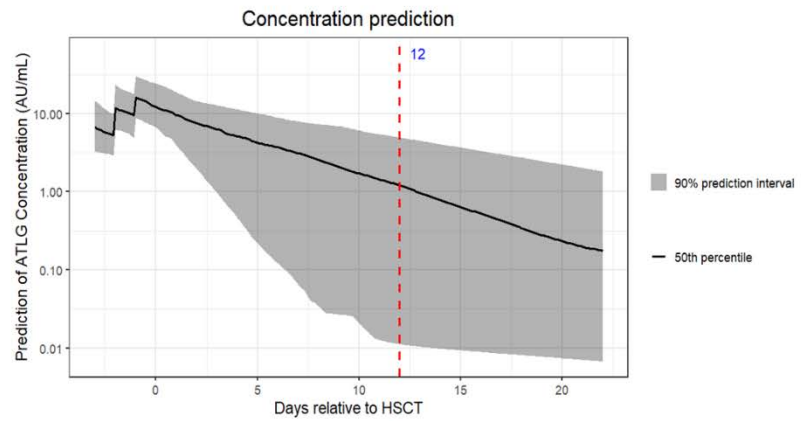
Number of doses (times)

Cumulative dose (mg/kg)

Infusion hours (hrs)

Time between first infusion and HSCT (days)

Plot in log scale  
 Yes  
 No



## D ATLG Population PK Model Simulation

Patient characteristics:

Weight of patient (kg)

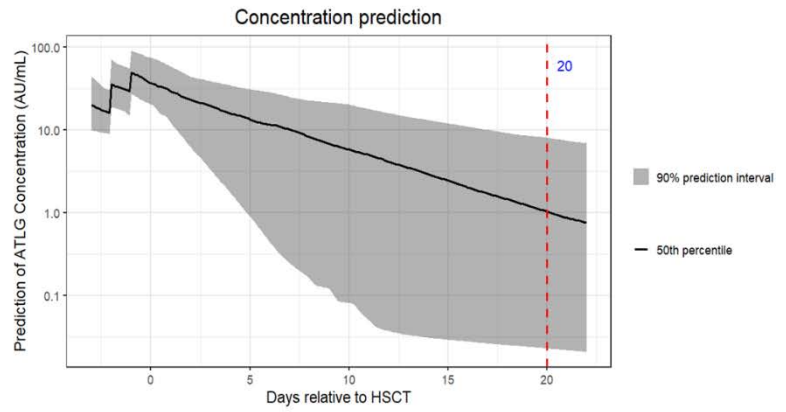
Number of doses (times)

Cumulative dose (mg/kg)

Infusion hours (hrs)

Time between first infusion and HSCT (days)

Plot in log scale  
 Yes  
 No



## References

- 1 Oostenbrink LVE, Jol-van der Zijde CM, Kielsen K, et al. Differential Elimination of Anti-Thymocyte Globulin of Fresenius and Genzyme Impacts T-Cell Reconstitution After Haematopoietic Stem Cell Transplantation. *Front Immunol* 2019; 10: 1–11.
- 2 Willemsen L, Jol-van der Zijde CM, Admiraal R, et al. Impact of serotherapy on immune reconstitution and survival outcomes after stem cell transplantations in children: thymoglobulin versus alemtuzumab. *Biol Blood Marrow Transplant* 2015; 21: 473–482.
- 3 Popow I, Leitner J, Grabmeier-Pfistershammer K, et al. A comprehensive and quantitative analysis of the major specificities in rabbit antithymocyte globulin preparations. *Am J Transplant* 2013; 13: 3103–3113.
- 4 Beal S, Sheiner L, Boeckmann A. NONMEM user's guides (1989-2009). Ellicott ICON Dev Solut 2006.
- 5 Jonsson EN, Karlsson MO. Xpose - An S-PLUS based population pharmacokinetic/pharmacodynamic model building aid for NONMEM. *Comput Methods Programs Biomed* 1998; 58: 51–64.
- 6 Lindbom L, Pihlgren P, Jonsson N. PsN-Toolkit - A collection of computer intensive statistical methods for non-linear mixed effect modeling using NONMEM. *Comput Methods Programs Biomed* 2005; 79: 241–257.
- 7 Keizer RJ, van Benten M, Beijnen JH, Schellens JHM, Huitema ADR. Piraña and PCluster: A modeling environment and cluster infrastructure for NONMEM. *Comput Methods Programs Biomed* 2011; 101: 72–79.
- 8 Comets E, Brendel K, Mentré F. Computing normalised prediction distribution errors to evaluate nonlinear mixed-effect models: The npde add-on package for R. *Comput Methods Programs Biomed* 2008; 90: 154–166.
- 9 R Development Core Team. R: a language and environment for statistical computing. Vienna R Found Stat Comput 2013.
- 10 Keizer RJ, Huitema ADR, Damen CWN, Schellens JHM, Beijnen JH. Farmacokinetiek van monoklonale antilichamen. *Ned Tijdschr Geneesk* 2007; 151: 683–688.
- 11 Efron B, Tibshirani R. Improvements on cross-validation: The .632+ bootstrap method. *J Am Stat Assoc* 1997; 92: 548–560.
- 12 Gerds TA, Kattan MW. *Medical Risk Prediction: With Ties to Machine Learning* (1st ed.). Chapman and Hall/CRC, 2021 DOI:<https://doi.org/10.1201/9781138384484>.

## Legend

**Individual plots per patient with observed and individual model predicted concentration-time curves – see separate additional pdf files.** For all patients we created 2 (normal and semi-log scale) individual plots with the observed concentrations (red dot) and model predicted ATLG concentration-time curves (blue line). Black dotted line is the lympholytic threshold of active ATLG of 1 arbitrary unit (AU)/mL. IPRED: individual predictions.

